Time-dependent models for dark matter at the galactic center

Gianfranco Bertone[1] and David Merritt[2]

[1]*NASA/Fermilab Theoretical Astrophysics Group, Batavia, Illinois 60510, USA*

[2]*Department of Physics, Rochester Institute of Technology, Rochester, New York 14623, USA*

(Received 26 January 2005; revised manuscript received 19 May 2005; published 4 November 2005)

The prospects for indirect detection of dark matter at the galactic center with γ-ray experiments like the space telescope GLAST, and air Cherenkov telescopes like HESS, CANGAROO, MAGIC and VERITAS depend sensitively on the mass profile within the inner parsec. We calculate the distribution of dark matter on subparsec scales by integrating the time-dependent Fokker-Planck equation, including the effects of self-annihilations, scattering of dark matter particles by stars, and capture in the supermassive black hole. We consider a variety of initial dark matter distributions, including models with very high densities (''spikes'') near the black hole, and models with ''adiabatic compression'' of the baryons. The annihilation signal after 10^{10} yr is found to be substantially reduced from its initial value, but in dark matter models with an initial spike, order-of-magnitude enhancements can persist compared with the rate in spike-free models.

DOI: 10.1103/PhysRevD.72.103502 PACS numbers: 95.35.+d, 97.60.Lf, 98.35.Gi

There is compelling evidence that the matter density of the Universe is dominated by some sort of nonbaryonic, ''dark'' matter (DM), the best candidates being weakly interacting massive particles [1,2]. Numerical N-body simulations suggest dark matter density profiles following broken power laws, $\rho \propto r^{-\gamma}$, with $\gamma \approx 3$ in the outer parts of halos and $1 \lesssim \gamma \lesssim 1.5$ (''cusps'') inside the solar circle. Although these profiles reproduce with sufficiently good accuracy the observed properties of galactic halos on large scales, as inferred by rotation curves, little is known about the DM distribution on smaller scales, where the gravitational potential is dominated by baryons. The situation at the galactic center (GC) is further complicated by the presence of a supermassive black hole (SBH), with mass $\sim 10^{6.5} M_\odot$ [3], whose sphere of gravitational influence extends out to ~ 1 pc.

The prospects for indirect detection depend crucially on the distribution of DM within this small region. The flux of γ rays from the GC, from the annihilation of DM particles of mass m and annihilation cross section in the nonrelativistic limit σv, can be written

$$\Phi_i(\Delta\Omega, E) \simeq \Phi_0 \frac{dN_i}{dE} \left(\frac{\sigma v}{\langle \sigma v \rangle_{\rm th}}\right) \left(\frac{1\ {\rm TeV}}{m}\right)^2 \overline{J}_{\Delta\Omega} \Delta\Omega \qquad (1)$$

where $\Phi_0 = 5.6 \times 10^{-12}\ {\rm cm}^{-2}\,{\rm s}^{-1}$ and $\langle \sigma v \rangle_{\rm th} = 3 \times 10^{-26}\ {\rm cm}^3\,{\rm s}^{-1}$ is the value of the thermally averaged cross section at decoupling that reproduces the observed cosmological abundance of dark matter (although in the presence of resonance effects like coannihilations, the correct relic abundance can be achieved with smaller cross sections). For more details and a review on DM candidates and detection see e.g. Refs. [1,2]. $\overline{J}_{\Delta\Omega}$ is a factor containing all the information on the DM profile [4]:

$$\overline{J}_{\Delta\Omega} \equiv K(\Delta\Omega)^{-1} \int_{\Delta\Omega} d\psi \int_\psi \rho^2 dl, \qquad (2)$$

where dl is the distance element along the line of sight at angle ψ with respect to the GC, $\Delta\Omega$ is the solid angle of the detector, and K is a normalizing factor, $K^{-1} = (8.5\ {\rm kpc}) \times (0.3\ {\rm GeV/cm}^3)^2$. We denote by $\overline{J}_5$ and $\overline{J}_3$ the values of $\overline{J}$ when $\Delta\Omega = 10^{-5}$ sr and 10^{-3} sr respectively; the former is the approximate field of view of the detectors in GLAST [5] and in atmospheric Cerenkov telescopes like VERITAS [6] and HESS [7], while the larger angle corresponds approximately to EGRET [8]. DM densities that rise more steeply than $\rho \propto r^{-3/2}$ near the GC imply formally divergent values of $\overline{J}$, hence the predicted flux of annihilation products can depend sensitively on any physical processes that modify the DM density on subparsec scales. Although the analysis of DM indirect detection is usually performed under simplifying assumptions on the DM profile—extrapolating the results of numerical simulations with power laws down to subparsec scales—several dynamical processes may influence the distribution of DM at the GC, including the gravitational force from the SBH [9], adiabatic compression of baryons [10], and heating of the DM by stars [11].

Here, we focus on the evolution of the annihilation signal due to two physical processes that are almost certain to strongly influence the form of the DM density profile near the GC: DM self-annihilations; and gravitational interactions between DM particles and stars. Both processes act on a similar time scale ($\sim 10^9$ yr) to modify $\rho(r)$ on the subparsec scales that are most relevant to the indirect detection problem. While these two mechanisms both tend to lower the DM density, we find that interestingly high densities can persist over a particular range of $(m, \sigma v)$ values. The time-dependent profiles discussed here may also have important consequences for the prospects of observing an extra-galactic γ-ray background.

Let $f(\mathbf{r}, \mathbf{v}, t)$ be the mass density of DM particles in phase space and $\rho(r, t)$ their configuration-space density, with r the distance from the GC, i.e. the distance from the SBH. We assume an isotropic velocity distribution,

$f(\mathbf{r}, \mathbf{v}, t) = f(E, t)$, where $E \equiv -v^2/2 + \phi(r)$ is the binding energy per unit mass and $-\phi(r)$ is the gravitational potential, which includes contributions from the stars in the galactic bulge and from the SBH. We assume that ϕ is fixed in time, i.e. that the mass of the SBH has not changed since the epoch of cusp formation, and that the stellar distribution has also not evolved. The first assumption is commonly made based on the observed, very early formation of massive black holes (e.g. [12]). The second assumption is motivated by the expectation that the stars should reach a collisional steady state around the SBH, the so-called "Bahcall-Wolf" solution [13], in a time of $\sim 10^9$ yr. The observed stellar distribution at the galactic center, $\rho_\star \sim r^{-1.4}$ [14], is slightly shallower than the Bahcall-Wolf solution for a single population but is generally believed to be consistent with a collisional steady state given uncertainties about the stellar mass spectrum [15]. We accordingly set $\rho_\star(r) \propto r^{-1.4}$ and fix its normalization to match the observed stellar density at ~ 1 pc from the SBH [14]. The stellar phase-space mass density $f_\star(E)$ is then uniquely determined by $\rho_\star(r)$ and $\phi(r)$ via Eddington's formula [16,17].

We describe the evolution of f via the orbit-averaged Fokker-Planck equation including loss terms (e.g. [18]):

$$\frac{\partial f}{\partial t} = \frac{1}{4\pi^2 p}\frac{\partial}{\partial E}\left[D_{EE}\frac{\partial f}{\partial E}\right] - f(E,t)\nu_{\rm coll}(E) - f(E,t)\nu_{\rm lc}(E), \tag{3a}$$

$$D_{EE}(E) = 64\pi^4 G^2 \overline{m}_\star \ln\Lambda\left[q(E)\int_{-\infty}^{E} dE' f_\star(E') + \int_E^\infty dE' q(E') f_\star(E')\right]. \tag{3b}$$

Here $p(E) = 4\sqrt{2}\int_0^{r_{\rm max}(E)} dr r^2\sqrt{\phi(r) - E}$ is the phase-space volume accessible per unit of energy, $p(E) = -\partial q/\partial E$, and $\ln\Lambda$ is the Coulomb logarithm [18]. We have assumed that the spectrum of stellar masses $n(m_\star)dm_\star$ is independent of radius; then $\overline{m}_\star = \langle m_\star^2\rangle/\langle m_\star\rangle$ [11].

The first term on the right-hand side of Eq. (3a) describes the diffusion of DM particles in energy space due to heating via gravitational encounters with stars. Near the SBH, the characteristic heating time is nearly independent of energy and radius and is given approximately by $T_{\rm heat} = 1.25\times 10^9\ {\rm yr}\tilde{M}_\bullet{}^{+1/2}\tilde{r}_h{}^{3/2}\tilde{m}_\star{}^{-1}$ with $\tilde{M}_\bullet = M_\bullet/(3\times 10^6 M_\odot)$; $\tilde{r}_h = r_h/(2\ {\rm pc})$, where r_h is the "gravitational influence radius" of the SBH, defined as the radius of the sphere containing a mass in stars equal to twice $M_\bullet$; and $\tilde{m}_\star = \overline{m}_\star/M_\odot$ [11]. In what follows we set $\tilde{M}_\bullet = \tilde{r}_h = \tilde{m}_\star = 1$ and define $\tau \equiv t/T_{\rm heat}$; the age of the galactic bulge, ~ 10 Gyr, then corresponds to $\tau \approx 10$. (The most recent estimates of $M_\bullet$ are slightly higher [19]; we adopt $\tilde{M}_\bullet = 1$ for consistency with earlier work [11].)

The collision term $\nu_{\rm coll}$ has two potential contributors: self-annihilations, and interaction of DM particles with baryons. The self-annihilation term is given locally by $\nu = m^{-1}\rho\sigma v$. The orbit-averaged rate $\nu_{\rm coll}$ that appears in Eq. (3a) is

$$\nu_{\rm coll}(E) = \frac{\int \nu r^2 v(r,E) dr}{\int r^2 v(r,E) dr} \tag{4}$$

where $v(r,E) = \sqrt{2(\phi(r) - E)}$ and the integrals are from 0 to $r_{\rm max}(E)$. Expressing ρ in terms of f, we can write the orbit-averaged self-annihilation term as

$$p(E)\nu_{\rm coll}(E) = 32\pi(\sigma v)m^{-1}\left[\int_0^E dE' f(E') C(E,E') \times \int_E^\infty dE' f(E') C(E',E)\right], \tag{5a}$$

$$C(E,E') \equiv \int_0^{\phi^{-1}(E)} dr r^2\sqrt{\phi(r) - E}\sqrt{\phi(r) - E'}. \tag{5b}$$

Self-annihilations limit the DM density roughly to $\rho \approx m/(\sigma v)t$ [9,20]; for $m = 50$ GeV, $\sigma v = 10^{-26}\ {\rm cm^3\ s^{-1}}$ and $t = 10$ Gyr, $\rho \lesssim 2\times 10^6 M_\odot\ {\rm pc}^{-3}$, which would imply that self-annihilations are important at $r \lesssim 10^{-3}$ pc if $\rho \sim r^{-3/2}$ and $\rho(r_h) = 100 M_\odot\ {\rm pc}^{-3}$.

The final loss term in Eq. (3) represents scattering of DM particles into the SBH [11]. This term, which we include, is important at radii $r \lesssim r_h$. The loss rate varies only logarithmically with the SBH's capture radius, which we set to $2GM_\bullet/c^2$.

In what follows, we assume $\tilde{m}_\star = 1 M_\odot$, consistent with our limited knowledge of the stellar mass spectrum near the galactic center [11]. We note that both the first and third terms on the right-hand side of Eq. (3a) depend in the same way on $\tilde{m}_\star$; thus, varying $\tilde{m}_\star$ has the effect of changing the relative time scales for DM-star scattering and self-annihilations. Since changing σv has the same effect, we do not vary $\tilde{m}_\star$ in what follows.

Equation (3) was advanced in time via a backward differentiation scheme coupled with the method of lines to reduce the partial differential equation to a system of ordinary differential equations [21]. A variable time step was employed, such that the fractional change in f in one time step was less than 1% at every value of E. For very high values of $\sigma v/m$, the initial f was truncated such that the annihilation time was never shorter than $\sim 10^6$ yr.

We adopted a wide range of initial conditions for the DM distribution (Table I). Baryon-free simulations of DM clustering suggest a power-law distribution in the inner parts of galaxies, $\rho \propto r^{-\gamma_c}$, a cusp, with $\gamma_c \approx 1$ [22] (these models are labeled N in Table I). The most recent simulations [23,24] (see also Refs. [25,26]) suggest a power-law index that varies slowly with radius, but the normalization and slope of these models at $r \approx r_h$ are essentially identical to those of models with an unbroken, $\rho \propto r^{-1}$ power law inward of the sun. We took $R_\odot = 8.0$ kpc for the radius of the solar circle [27].

TABLE I. Properties of the halo models. N and A stand for Navarro, Frenk, and White and adiabatically contracted profiles, respectively. The subscripts c, "sp" are for profiles with core and spike, respectively. Core radius r_c is in units of r_h. Density at $R_\odot$ is in units of GeV cm^{-3}. $\overline{J}_3$ and $\overline{J}_5$ are values of J averaged over windows of solid angle 10^{-3} and 10^{-5} sr respectively and normalized as described in the text. The final two columns give $\overline{J}$ in evolved models for $\sigma v = 0$ (no annihilations), and for $(\sigma v, m) = (3 \times 10^{-26}\ \mathrm{cm}^3\ \mathrm{s}^{-1}, 50\ \mathrm{GeV})$ (maximal annihilation rate), respectively.

	γ_c	$\gamma_{\rm sp}$	r_c	$\rho(R_\odot)$	$\log_{10}\overline{J}_3$ ($\overline{J}_5$) $\tau = 0$	$\tau = 10$	$\tau = 10$
N	1.0	...	...	0.3	2.56 (3.51)	2.56 (3.50)	2.56 (3.50)
N_c	1.0	...	10	0.3	2.54 (3.33)	2.54 (3.33)	2.54 (3.33)
$N_{\rm sp}$	1.0	2.33	...	0.3	9.21 (11.2)	3.86 (5.84)	2.56 (3.52)
$N_{c,\rm sp}$	1.0	2.29	10	0.3	6.98 (8.98)	2.61 (3.88)	2.54 (3.33)
A	1.5	...	...	0.5	5.80 (7.75)	5.26 (7.03)	5.23 (6.98)
A_c	1.5	...	10	0.5	4.96 (6.27)	4.96 (6.27)	4.96 (6.27)
$A_{\rm sp}$	1.5	2.40	...	0.5	14.8 (16.8)	9.25 (11.3)	5.25 (7.02)
$A_{c,\rm sp}$	1.5	2.29	10	0.5	9.99 (12.0)	5.21 (6.96)	4.96 (6.27)

Since the total mass budget of the inner Galaxy is dominated by baryons, the DM distribution is likely to have been influenced by the baryonic potential and its changes over time. The "adiabatic-growth" model [10] posits that the baryons contracted quasistatically and symmetrically within the preexisting DM halo, pulling in the DM and increasing its density. When applied to a DM halo with initial $\gamma_c \approx 1$, the result is a halo profile with $\gamma_c \approx 1.5$ inward of $R_\odot$ and an increased density at $R_\odot$ [28–30]. Adiabatically contracted halo models are labeled A in Table I. Alternatively, strong departures from spherical symmetry during galaxy formation might have resulted in a *lower* central DM density. For instance, the DM density following a merger is a weak power law, $\rho \sim r^{-\gamma_{\rm in}}$, $\gamma_{\rm in} \approx 0.5$, inside a radius $r_c \approx 10 - 100 r_h$ [31,32]. Models with the subscript c in Table I have $\rho \propto r^{-1/2}$ inside a radius $r_c = 10$ pc.

We also considered modified versions of each of these DM profiles that included a density spike around the SBH; these models are denoted by the subscript "sp" in Table I. The inner DM density in the spike models follows the steeper power law that would result from gradual growth of the SBH to its current mass at a fixed location. We set $\rho = \rho(r_b)(r/r_b)^{-\gamma_{\rm sp}}$ for $r \lesssim r_b$ with $\gamma_{\rm sp} = 2 + 1/(4 - \gamma)$ and γ the power-law index of the core or cusp, and $r_b = 0.2 r_h$ [9,33]. It is unclear whether spikes can survive at the centers of all galactic halos, since dynamical effects such as off-center formation of the SBH and binary black hole mergers would tend to destroy high density regions [31,32]. However, the Milky Way is unlikely to have experienced a "major merger" (a merger with another galaxy of comparable mass) in the last 10 Gyr, and the existence of a stellar cusp [14] further strengthens the case for a dark matter spike at the galactic center [34].

In order to evaluate the influence of annihilations on the evolution of the DM profile, we first investigated two extreme cases in the framework of typical DM candidates like neutralinos or Kaluza-Klein (KK) particles [1]. In the first extreme case, in order to maximize the ratio $\sigma v/m$, we assumed a cross section $\sigma v = \langle \sigma v \rangle_{\rm th} = 3 \times 10^{-26}\ \mathrm{cm}^3\ \mathrm{s}^{-1}$ and a mass of 50 GeV. Higher values of the annihilation cross section, though possible, would imply a low relic density, making the candidate a subdominant component of the DM in the Universe, a case we are not interested in here. The lower limit on the mass strictly applies only to neutralinos in theories with gaugino and sfermion mass unification at the grand unified theory scale [35], while the limit on the mass of KK particles is higher. The second extreme case assumes no annihilations, as in the limit of very small cross sections, or very heavy particles. Table I gives values of $\overline{J}_3$ and $\overline{J}_5$ at $\tau = 10$ for each of our DM models and for both of the extreme particle physics models. The $\overline{J}$ values depend appreciably on the particle physics model only when the initial DM density has a spike around the SBH; in other cases the central density is too low for annihilations to affect $\overline{J}$. Particularly in the case of maximal σv, the final $\overline{J}$ values are found to be modest, $\log_{10}\overline{J}_3 \lesssim 5.3$ and $\log_{10}\overline{J}_5 \lesssim 7.0$, compared with the much larger values at $\tau = 0$ in the presence of spikes.

We also carried out integrations for the set of benchmark models derived in [36] in the framework of minimal supergravity. Although other scenarios (supersymmetric or not) predict different parameters for the DM candidate, the values of $\sigma v/m$ are often approximately the same. Light DM candidates [37], for example, have masses smaller than 20 MeV if they are to be responsible for the 511 keV emission from the galactic bulge [38], but they also typically have cross sections much smaller than the thermal cross section in the early Universe, which implies that $\sigma v/m$ falls again in the same range discussed above. Heavy candidates, like those proposed to explain the HESS data [39,40], have masses in the 10–20 TeV range, and thermal cross sections, so that they fall again in the same range of $\sigma v/m$. Figure 1 shows the final DM density profile for each of the benchmark models, starting from DM models $N_{\rm sp}$ and $A_{\rm sp}$; the latter model is the "adiabatically contracted" version of the former. While adopting the maximal annihilation rate effectively destroys the spike and produces $\overline{J}$ values as low as those of spike-free models, other benchmark models with smaller $\sigma v/m$ result in strong enhancements in $\overline{J}$.

Figure 2 shows the evolution of the dark matter density at a radius of $10^{-5} r_h \approx 2 \times 10^{-5}$ pc, starting from a $\rho \sim r^{-2.33}$ spike ($\rho \sim r^{-1}$ cusp). Two values were taken for the initial density normalization at $r = r_h$, $\rho(r_h) = (10, 100) M_\odot\ \mathrm{pc}^{-3}$. The self-annihilation term in Eq. (3a) was computed assuming $m = 200$ GeV, $\sigma v = 10^{-27}\ \mathrm{cm}^3\ \mathrm{s}^{-1}$. The early evolution is dominated by self-

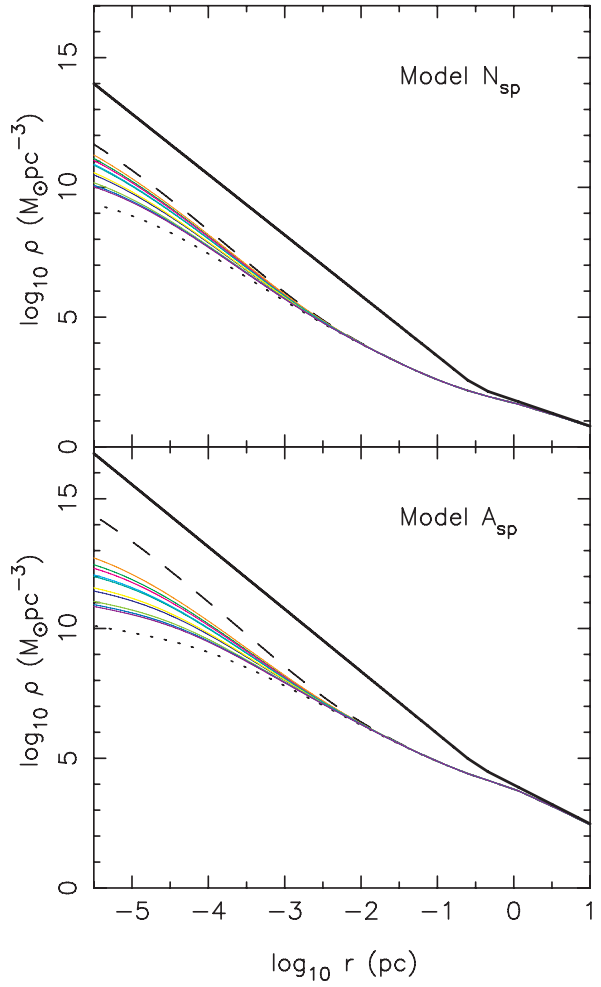

FIG. 1 (color). Evolved DM density profiles at $\tau = 10$ (roughly 10^{10} yr) starting from two initial DM profiles (see Table I and text). Colored curves: benchmark models; dashed lines: $\sigma v = 0$; dotted curves: $\sigma v = 3 \times 10^{-26}$ cm^3 s^{-1}, $m =$ 50 GeV; thick lines: initial DM density.

annihilations but for $t \gtrsim 10^9$ yr $\approx T_{\rm heat}$, heating of dark matter by stars dominates. The change in $\overline{J}_5$ [Fig. 2(b)] is dramatic, with final values in the range $10^3 \lesssim \overline{J} \lesssim 10^5$.

We define the boost factor b as $\overline{J}/\overline{J}_N$, with $\overline{J}$ the value in the evolved model and $\overline{J}_N$ the value in a $\rho \propto r^{-1}$ (spike-free) halo with the same density normalization at $r = R_\odot$. Figure 3 shows boost factors at $\tau = 10$ for each of the models in Table I. We found that the dependence of $B \equiv \log_{10} b$ on $\sigma v/m$ could be very well approximated by the function

$$B(X) = B_{\rm max} - (1/2)(B_{\rm max} - B_{\rm min}) \times \{1 + \tanh[C_1(X - C_2)]\} \quad (6)$$

with $X \equiv \log_{10}(\sigma v/10^{-30}\ {\rm cm^3\,s^{-1}})/(m/100\ {\rm GeV})$. Table II gives values of the fitting parameters at $\tau = 10$ in each of the models with a spike. The boost factor is independent of σv for low σv, since annihilations are

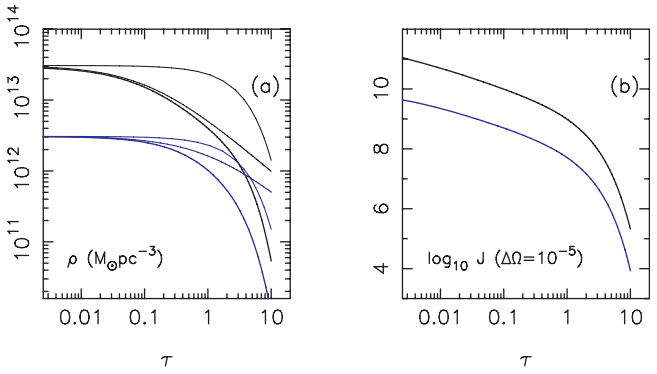

FIG. 2 (color). (a) Evolution of the dark matter density at a radius of $10^{-5} r_h \approx 2 \times 10^{-5}$ pc in a $\rho \sim r^{-2.33}$ spike, for $m =$ 200 GeV, and $\sigma v = 10^{-27}$ cm^3 s^{-1}. The upper (lower) set of curves corresponds to an initial density normalization at r_h of $10(100) M_\odot$ pc^{-3}. In order of increasing thickness, the curves show the evolution of ρ in response to heating by stars; to self-annihilations; and to both processes acting together. Time is in units of $T_{\rm heat}$ defined in the text; $\tau = 10$ corresponds roughly to 10^{10} yr. (b) Evolution of $\overline{J}$ averaged over an angular window of 10^{-5} sr.

unimportant in this limit, and also for high σv, since annihilations effectively destroy the spike.

We now apply these results to the study of high-energy γ rays from dark matter annihilations at the GC. An early detection by the EGRET Collaboration, of a γ-ray source coincident with the position of the SBH [41], has not been confirmed by a subsequent analysis [42]. However, air

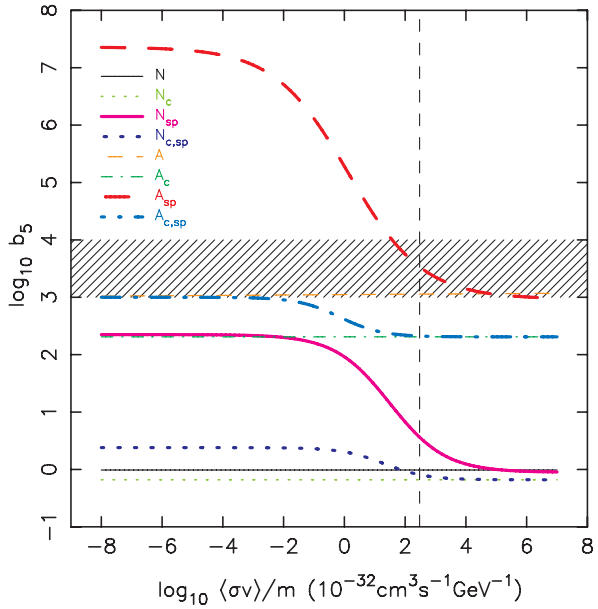

FIG. 3 (color). Boost factors b_5 ($\Delta\Omega = 10^{-5}$) as a function of $\sigma v/m$ at $\tau = 10$ for the DM models of Table I. The hatched region is the approximate boost factor required to explain the HESS γ-ray detection if the particle mass is $\sim$10 TeV and $\sigma v = 3 \times 10^{-26}$ cm^3 s^{-1} (vertical line).

TABLE II. Parameters in the fitting function for the boost.

$\Delta\Omega =$	10^{-3}				10^{-5}			
	$B_{\min}$	$B_{\max}$	C_1	C_2	$B_{\min}$	$B_{\max}$	C_1	C_2
$N_{\rm sp}$	−0.02	1.31	0.66	0.73	−0.05	2.35	0.55	1.50
$N_{c,\rm sp}$	−0.02	0.05	0.75	0.92	−0.18	0.38	0.72	1.31
$A_{\rm sp}$	2.16	6.29	0.43	−0.28	2.97	7.36	0.41	0.13
$A_{c,\rm sp}$	1.96	2.22	0.74	−0.49	2.31	3.00	0.72	−0.15

Cherenkov telescopes like HESS, CANGAROO and VERITAS have all detected a source coincident within their angular resolution with the GC SBH. In particular the HESS data suggest a spectrum extending up to 10 TeV, with no apparent cutoff [43]. It is difficult to interpret the observed emission as due to DM annihilation, since usual DM candidates are lighter than the required 10 TeV, and since the spectrum is quite flat. The latter problem can be solved by considering processes like $\chi\chi \to \ell\bar{\ell}\gamma$ [39], where ℓ is a charged lepton, a channel heavily suppressed for neutralinos, but open for Kaluza-Klein particles. Although the contribution of the total flux is small (the channel is suppressed by a factor α/π with respect to the annihilation to charged leptons), the corresponding photon spectrum is very flat, with a sharp cutoff at an energy corresponding to the particle mass. The other problem, i.e. the high dark matter particle mass required to reproduce the HESS data, can be solved in the framework of some specific theoretical scenarios, such as those proposed in Refs. [39,40]. In this case, a boost factor of order $10^3 \lesssim b \lesssim 10^4$ is required to match the observed normalization, for particle masses of order 10 TeV and cross sections of order 3×10^{-26} cm^3 s^{-1}. Figure 2 shows that such boost factors are achievable in the adiabatically compressed DM models, $\rho \sim r^{-1.5}$, especially if a spike is initially present, although the spike is not required. We note that the particle models discussed above could easily evade the synchrotron constraints discussed in [44–46]. Looking, for example, at Fig. 6 of Ref. [46], we note that the synchrotron constraint is weaker for heavier masses, and the annihilation rate, in the case of the evolved $A_{\rm sp}$ profile discussed above, is suppressed by many orders of magnitude with respect to the case discussed in [46], corresponding to a nonevolved $N_{\rm sp}$ profile (Table I). A detailed analysis of indirect detection of supersymmetric and Kaluza-Klein DM in light of this work will be presented elsewhere.

This work was supported by Grants No. AST-0071099, No. AST-0206031, No. AST-0420920 and AST-0437519 from the NSF, Grants No. NNG04GJ48G and No. NAG 5-10842 from NASA, and Grant No. HST-AR-09519.01-A from STScI.

[1] G. Bertone, D. Hooper, and J. Silk, Phys. Rep. **405**, 279 (2005).
[2] L. Bergstrom, Rep. Prog. Phys. **63**, 793 (2000).
[3] R. Schödel, T. Ott, R. Genzel, A. Eckart, N. Mouawad, and T. Alexander, Astrophys. J. **596**, 1015 (2003).
[4] L. Bergstrom, P. Ullio, and J. H. Buckley, Astropart. Phys. **9**, 137 (1998).
[5] http://www-glast.stanford.edu/
[6] http://veritas.sao.arizona.edu/
[7] http://www.mpi-hd.mpg.de/hfm/HESS/HESS.html/
[8] http://cossc.gsfc.nasa.gov/egret/
[9] P. Gondolo and J. Silk, Phys. Rev. Lett. **83**, 1719 (1999).
[10] G. R. Blumenthal, S. M. Faber, R. Flores, and J. R. Primack, Astrophys. J. **301**, 27 (1986).
[11] D. Merritt, Phys. Rev. Lett. **92**, 201304 (2004).
[12] X. Fan *et al.*, Astron. J. **128**, 515 (2004).
[13] J. N. Bahcall and R. A. Wolf, Astrophys. J. **209**, 214 (1976).
[14] R. Genzel *et al.*, Astrophys. J. **594**, 812 (2003).
[15] T. Alexander, Astrophys. J. **527**, 835 (1999).
[16] A. S. Eddington, Mon. Not. R. Astron. Soc. **76**, 572 (1916).
[17] P. Gondolo and J. Silk, Phys. Rev. Lett. **83**, 1719 (1999).
[18] L. Spitzer, *Dynamical Evolution of Globular Clusters* (Princeton University Press, Princeton, NJ, 1987).
[19] A. M. Ghez *et al.*, Astrophys. J. **620**, 744 (2005).
[20] V. S. Berezinsky, A. V. Gurevich, and K. P. Zybin, Phys. Lett. B **294**, 221 (1992).
[21] M. Berzins, P. M. Dew, and R. M. Furzeland, Appl. Numer. Math. **5**, 375 (1989).
[22] J. F. Navarro, C. S. Frenk, and S. D. M. White, Astrophys. J. **462**, 563 (1996).
[23] J. F. Navarro *et al.*, Mon. Not. R. Astron. Soc. **349**, 1039 (2004).
[24] D. Reed, F. Governato, L. Verde, J. Gardner, T. Quinn, J. Stadel, D. Merritt, and G. Lake, Mon. Not. R. Astron. Soc. **357**, 82 (2005).
[25] T. Fukushige, A. Kawai, and J. Makino, Astrophys. J. **606**, 625 (2004).
[26] J. Diemand, B. Moore, and J. Stadel, Mon. Not. R. Astron. Soc. **353**, 624 (2004).
[27] F. Eisenhauer *et al.*, Astrophys. J. **597**, L121 (2003).
[28] J. Edsjo, M. Schelke, and P. Ullio, J. Cosmol. Astropart. Phys. 09 (2004) 004.
[29] F. Prada, A. Klypin, J. Flix, M. Martinez, and E. Simonneau, Phys. Rev. Lett. **93**, 241301 (2004).
[30] O. Y. Gnedin, A. V. Kravtsov, A. A. Klypin, and D. Nagai, Astrophys. J. **616**, 16 (2004).
[31] D. Merritt, M. Milosavljevic, L. Verde, and R. Jimenez, Phys. Rev. Lett. **88**, 191301 (2002).
[32] P. Ullio, H. Zhao, and M. Kamionkowski, Phys. Rev. D **64**, 043504 (2001).

[33] D. Merritt, in *Coevolution of Black Holes and Galaxies*, edited by L. C. Ho, Carnegie Observatories Astrophysics Vol. 1 (Cambridge University Press, Cambridge, UK, 2004), p. 100.
[34] J. Silk, Int. J. Mod. Phys. A **17**, 167 (2002).
[35] S. Eidelman *et al.*, Phys. Lett. B **592**, 1 (2004).
[36] M. Battaglia, A. De Roeck, J. R. Ellis, F. Gianotti, K. A. Olive, and L. Pape, Eur. Phys. J. C **33**, 273 (2004).
[37] C. Boehm, D. Hooper, J. Silk, and M. Casse, Phys. Rev. Lett. **92**, 101301 (2004).
[38] J. F. Beacom, N. F. Bell, and G. Bertone, Phys. Rev. Lett. **94**, 171301 (2005).
[39] L. Bergstrom, T. Bringmann, M. Eriksson, and M. Gustafsson, Phys. Rev. Lett. **94**, 131301 (2005).
[40] D. Hooper and J. March-Russell, Phys. Lett. B **608**, 17 (2005).
[41] H. A. Mayer-Haesselwander *et al.*, Astron. Astrophys. **335**, 161 (1998).
[42] D. Hooper and B. L. Dingus, Phys. Rev. D **70**, 113007 (2004).
[43] F. Aharonian *et al.*, Astron. Astrophys. **425**, L13 (2004).
[44] G. Bertone, G. Sigl, and J. Silk, Mon. Not. R. Astron. Soc. **326**, 799 (2001).
[45] P. Gondolo, Phys. Lett. B **494**, 181 (2000).
[46] R. Aloisio, P. Blasi, and A. V. Olinto, J. Cosmol. Astropart. Phys. 05 (2004) 007.